Thermochimica Acta, 194 (1992) 47–58
Elsevier Science Publishers B.V., Amsterdam

A mechanistic investigation and kinetic analysis of the thermal decomposition of diammonium hexanitrato cerate catalysed by $Cd_xCo_{1-x}Fe_2O_4$ catalysts

R.M. Gabr, A.M. El-Awad and M.M. Girgis
Chemistry Department, Faculty of Science, Assiut University, Assiut (Egypt)

(Received 8 March 1991)

Abstract

The isothermal and non-isothermal decomposition of pure diammonium hexanitrato cerate(IV) and its mixtures with 10% (wt/wt) of $Cd_xCo_{1-x}Fe_2O_4$ catalysts ($x = 0.0$, 0.5 and 1.0) were investigated. The effect of catalyst additives on the kinetics of isothermal decomposition of the parent salt was also studied. Their isothermal curves of fraction decomposed (α) against time were sigmoid in nature and the decomposition reaction in the presence of these catalyst additives obeys the Avrami–Erofe'ev equation. Such catalytic pretreatment reduced the induction period to the onset of the reaction decomposition. From the complementary consideration of microscopic observations and kinetic evidence, we conclude that the thermal decomposition of the parent salt in the presence of these catalyst additives, in the temperature range 250–325 °C, proceeds by the nucleation-and-growth mechanism. The promotional effect of the catalysts used was also described. It can be stated that the activity of these catalysts in promoting salt breakdown is a consequence of their appreciable solubility in the parent salt and that the chemistry of the reaction in such conditions is complicated. It involves several participants, including the unstable ammine complexes of both Cd and Co ions, located in the octahedral sites of the catalysts, formed as intermediates of the type $[M(NH_3)_6]^{2+}$.

INTRODUCTION

Diammonium hexanitrato cerate(IV) (DAHC) is generally a parent precursor for the thermal genesis of pure ceric oxide catalyst. The preparation and characteristics of ceric oxide (ceria) are of great interest from the industrial point of view [1]. Ceria is an essential material in high-temperature fuel-cell applications [2,3]. It has been reported that ceric oxide exhibits a marked activity towards many catalytic reactions [4,5]. The structural characteristics and high thermal stability [6] of ceria, together with its n-semiconductive behaviour [7], support its industrial application as a catalyst. The main object of most kinetic studies is the determination of the reaction mechanism. For solid state decomposition, this usually involves investigation of any factors that may provide information concerning interface conditions and any participating intermediates [8]. Moreover,

studies of the influence of additives on salt decomposition processes are often directed towards the determination or confirmation of the decomposition mechanism of the pure compound [9].

The present article extends studies on the thermal decomposition of DAHC in order to investigate the role of $Cd_xCo_{1-x}Fe_2O_4$ catalysts in promoting the decomposition to CeO_2. Kinetic measurements of the isothermal decomposition of pure and mixed DAHC were analysed and the results were supported by microscopic observations. These data were discussed in terms of the chemistry [10] of the nucleation-and-growth mechanism, the central feature of the mechanistic interpretation of rate studies of solid-state reactions.

EXPERIMENTAL

All the reagents used in the present investigation were of analytical grade (BDH chemicals). The mixing of DAHC with 10% (wt/wt) $Cd_xCo_{1-x}Fe_2O_4$ catalysts ($x = 0.0$, 0.5 and 1.0) was carried out in an agate morter. TG and DSC curves were obtained using a 1090 Du Pont thermal analyser, with a heating rate 10 °C min^{-1}. The α–t data of the pure parent salt and its mixtures with the catalysts were obtained as described elsewhere [11] in the temperature range 250–325 °C. A Philips X-ray diffractometer (model PW 1710) was used to record d values, up to $2\theta = 80°$, for pure and mixed DAHC and their calcination products within the above temperature range. IR absorption spectra from thin discs of potassium bromide-supported test samples (< 1 wt.%) were recorded using a Perkin–Elmer 580 B spectrophotometer. Scanning electron microscopic (SEM) examinations were carried out using a JEOL 200 microscope (JEOL, Tokyo, Japan) operated to 15 keV to minimise specimen damage.

RESULTS AND DISCUSSION

TG curves for pure and mixed samples are presented in Fig. 1. Pure diammonium hexanitrato cerate [$(NH_4)_2Ce(NO_3)_6$], DAHC, decomposes in four steps, Fig. 1a. The DSC curve for the pure salt also exhibits four endothermic effects, see Fig. 2, their positions being equivalent to the corresponding TG stages. The first decomposition stage at 225–235 °C involves a weight loss of 3.9% which is slightly higher than that (3.1%) anticipated for the evolution of ammonia by the reaction

$$(NH_4)_2Ce(NO_3)_6 \rightarrow (NH_4)HCe(NO_3)_6 + NH_3 \quad (1)$$

The second endothermic decomposition step at 250–280 °C brings the total weight loss up to 22.9% and can be assigned to the transformation of $(NH_4)HCe(NO_3)_6$ to the oxynitrato intermediate $H_2CeO(NO_3)_4$ [12]. In this context, the XRD patterns (Fig. 3a) for the pure salt calcined at 250 °C

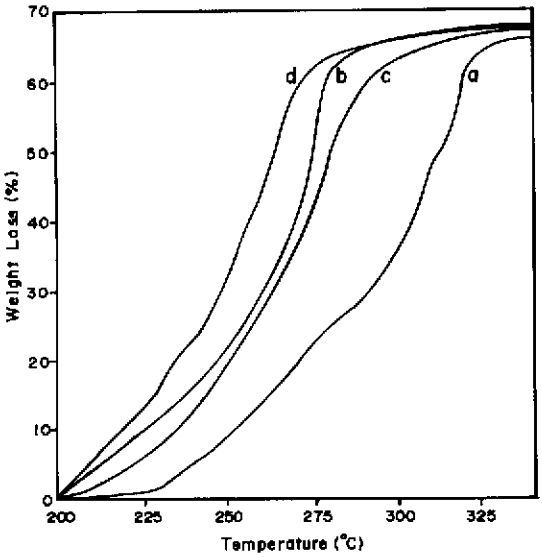

Fig. 1. TG curves for the non-isothermal decomposition of pure DAHC and its mixture with 10% (wt/wt) $CoFe_2O_4$, $CdFe_2O_4$ and $Cd_{0.5}Co_{0.5}Fe_2O_4$ (a–d respectively).

indicate a trace of CeO_2 together with the parent sample. In addition, the relevant IR spectrum of this sample (Fig. 4) shows noticeable changes in the characteristic band structure of the parent salt; these are the absorptions at 3145, 1470, 1400, 1320, 820 and 730 cm^{-1}, assigned to the

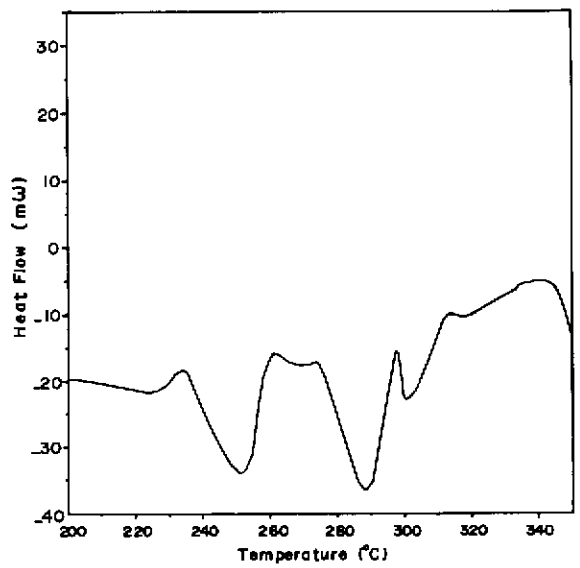

Fig. 2. DSC curve for the pure DAHC.

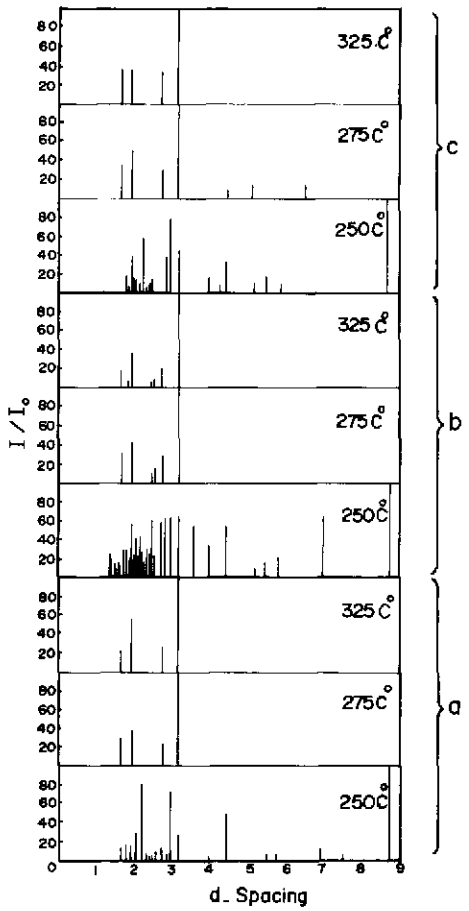

Fig. 3. XRD for pure DAHC and its mixtures with $CoFe_2O_4$ and $CdFe_2O_4$ (a–c respectively) and their calcination products.

symmetric ionic nitrates [13] and to the asymmetry appearing in the nitrate group as a result of an increase in the degree of covalency [14]. The appearance of an absorption emerging at 620–245 cm^{-1} for the sample calcined at 275 °C, is interpreted as "metal–oxygen"-type vibrations, i.e. Ce–O [12]. Moreover, the observed absorption bands at 480 and 350 cm^{-1} are higher than that reported [15] (345 cm^{-1}) for CeO_2, indicating a higher bond order for the Ce–O of the oxynitrato anion, confirming its double-bonding nature.

The total weight loss in the third stage (250–320 °C) amounts to 48.5%, which is very close to that (49%) anticipated theoretically for formation of the simple oxynitrate compound $CeO(NO_3)_3$. The IR spectrum of the parent sample calcined at 300 °C shows a reduction in the absorptions arising from the coordinated nitrates and the development of an absorption at 600–250 cm^{-1}, assigned to Ce=O. These two facts are consistent with

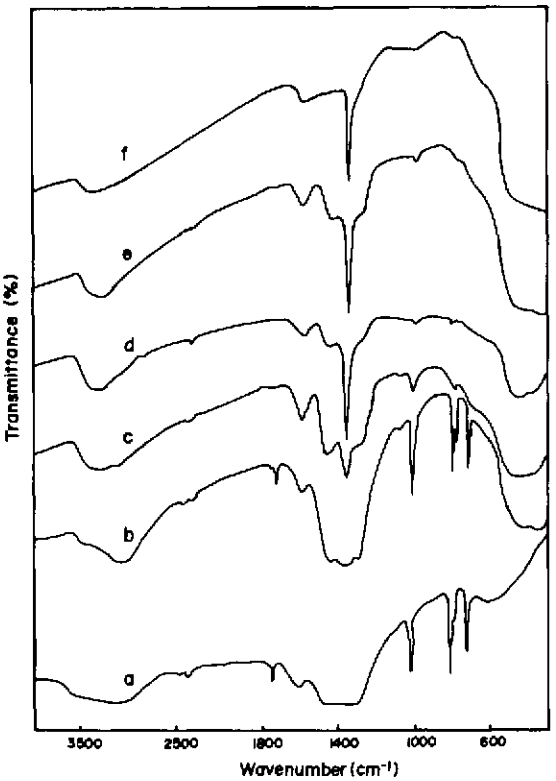

Fig. 4. Infrared absorption spectra of the parent pure DAHC and its calcination products at 250, 275, 300, 325 and 350 °C (a–f respectively).

the formation of the oxynitrate compound. Calculations based on the total weight loss (66.9%) following the final decomposition step (310–330 °C) suggest the formation of CeO_2 as a final product. This is corroborated by both the XRD patterns and the development of the IR spectra of the calcination products formed up to 350 °C, where a progressive increase in the intensity of the absorption at 345 cm^{-1} and a gradual diminution of the absorptions due to the different nitrate contributions were observed.

The kinetics of the isothermal measurements were undertaken to extend the systematic investigation of the decomposition of pure DAHC in the temperature range 250–325 °C. The curves of fraction decomposed (α) against time were characteristically sigmoid in shape and are represented in Fig. 5a. Analysis of the kinetic data was preceded by determining which rate equation, derived from different models [16], provided the most accurate fit of the experimental data (α, t). The computer-oriented kinetic analysis was carried out for each set of α and t values. The results showed that the Ginstling–Brounshtein equation gives the best fit of the data, with a correlation coefficient very close to unity. Accordingly, we can conclude that the salt breakdown is kinetically controlled by the diffusion of the

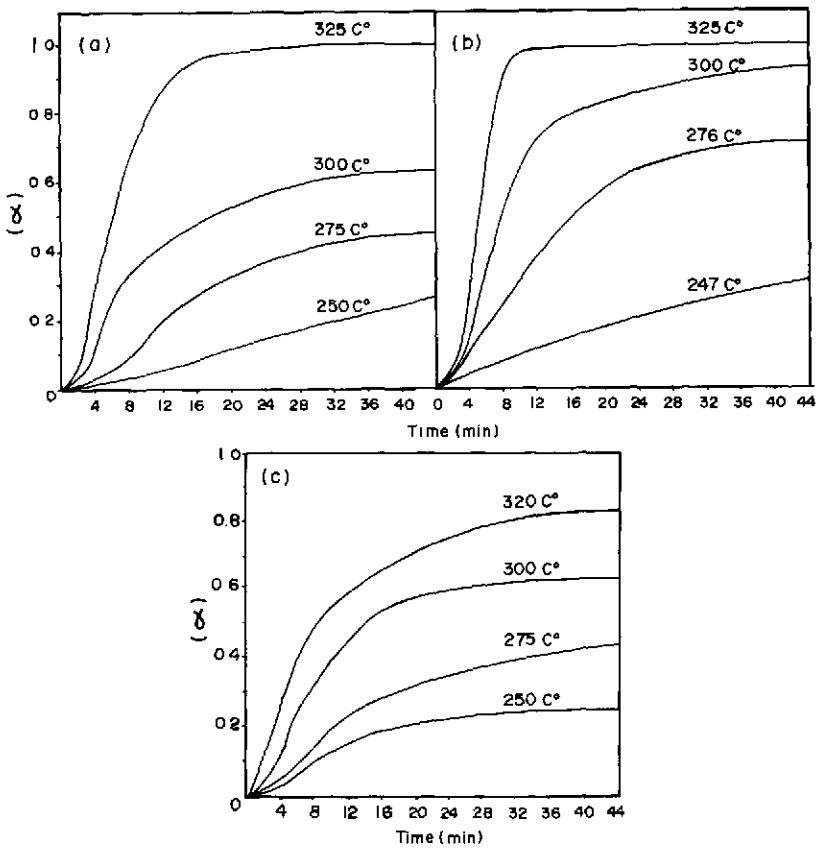

Fig. 5. α vs. time curves for the isothermal decomposition of pure DAHC and its mixtures with 10% (wt/wt) $CdFe_2O_4$ and $CoFe_2O_4$ (a–c respectively).

eventual gaseous reaction products (NH_3, N_2O or N_2O_5) along the interface between the reactant and solid product [17]. The activation energy E_a for the decomposition reaction was estimated as 89.88 kJ mol^{-1} from the rate constants measured between 250 and 325 °C and by applying the Arrhenius equation.

Kinetic evidence alone cannot provide positive proof of the operation of a particular mechanism. Conclusions concerning textural changes and/or the geometry of the interface advance should be supported by independent evidence, e.g. microscopic observations [18,19]. Therefore, SEM examinations, Fig. 6a–6d, were carried out for the parent DAHC calcinated at different decomposition temperatures. The SEM photograph for the sample heated at 250 °C shows a different morphology compared to that of the parent sample, the significant features being the formation of cracks and pores that probably arise as a consequence of the build-up of gas pressure (diffusion controlled) during the decomposition process. A noticeable development in porosity was detected on raising the decomposition tempera-

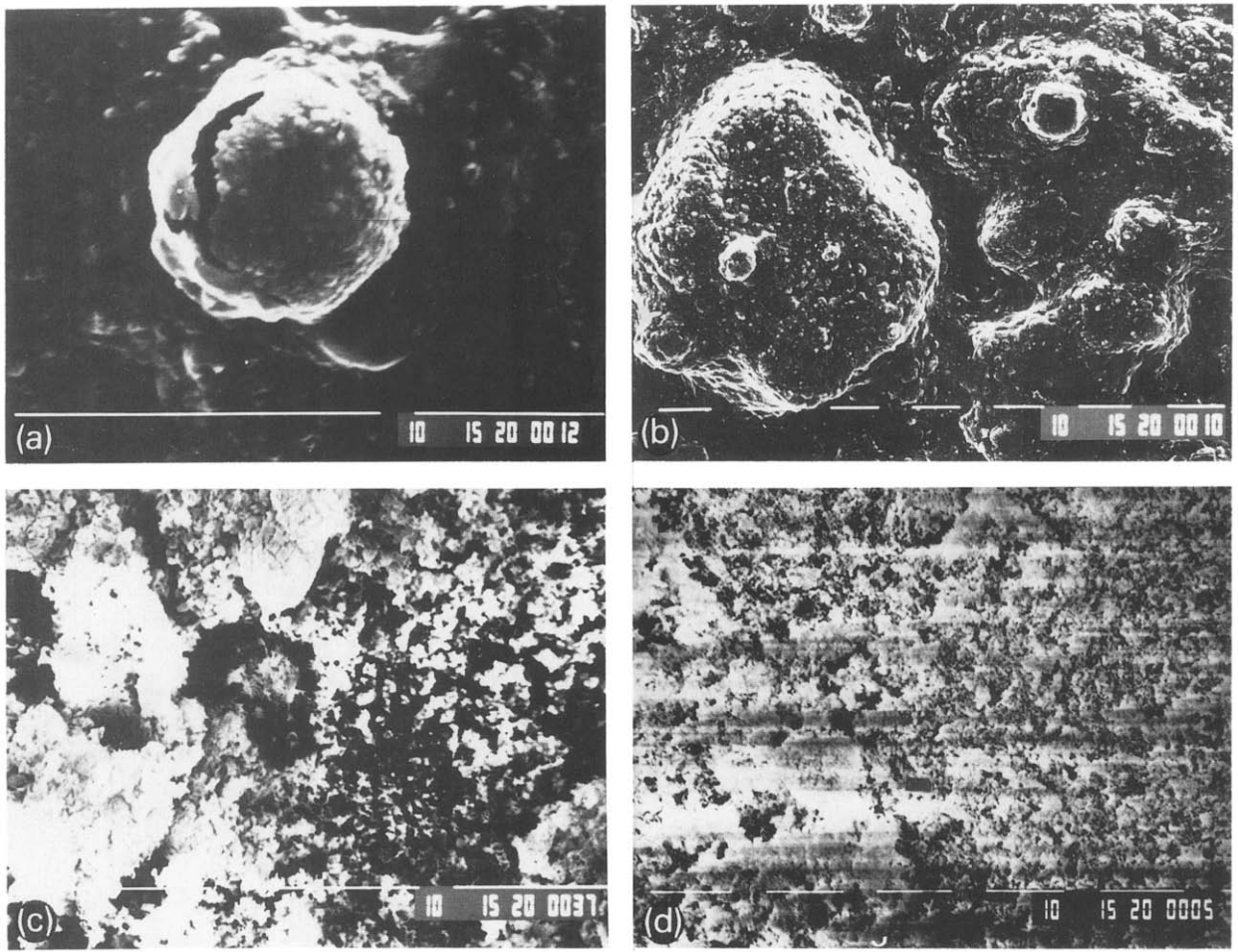

Fig. 6. Scanning electron micrographs for pure DAHC calcinated at 250, 275, 300 and 325 °C (a–d respectively).

ture up to 325 °C, where the structural coherency of the crystals was lost and the crystallites reacted to completion Fig. 6b–6d.

Studies of the influence of catalyst additives on the thermal behaviour of salt decomposition are often directed towards the formulation and/or confirmation of a mechanism for the decomposition of the pure compound. Such studies are frequently qualitative and kinetic conclusions may not extend beyond the comment that a particular additive accelerates, inhibits or is without influence on the decomposition process. Therefore, the thermal decomposition of pure DAHC was tested isothermally and non-isothermally in the presence of three catalysts of general formula $Cd_xCo_{1-x}Fe_2O_4$, with $x = 0.00$, 0.5 and 1.0. These catalysts were well characterised structurally and were pre-tested in another catalytic reaction [20]. Examination of the corresponding TG curves for DAHC mixed with $CoFe_2O_4$,$CdFe_2O_4$ and $Cd_{0.5}Co_{0.5}Fe_2O_4$ (Fig. 1b, 1c and 1d, respectively), shows that: all these catalysts accelerate the thermal decomposition of pure DAHC salt; there is a diminution of the induction period to the onset of the reaction decomposition; 10% (wt/wt) of $Cd_{0.5}Co_{0.5}Fe_2O_4$ has a remarkable promotional effect; and the multi-stage decomposition behaviour observed in pure DAHC does not take place in the presence of these catalysts. The above findings suggest that the mechanistic criteria of DAHC decomposition behave differently in the presence of catalyst additives. The disappearance of d spacing values characterising the ferrite structure in the DAHC–catalyst mixtures on raising the decomposition reaction temperature, indicates the appreciable solubility of the catalyst additives in the host matrix. This property enables the ammonia produced in the early stages of decomposition to react with the octahedrally active sites in the catalysts that are occupied by both Cd and Co ions, forming the less stable ammine complex [21,22]. Thus, the interaction of these complexes in the dissolved mixture accounts for the ability of these catalysts to promote decomposition by a route that does not involve the intervention of the other more stable intermediates formed in the case of the pure salt. Accordingly, decomposition proceeded more easily. The significant promotional effect arising in the case of catalyst with the composition $x = 0.5$ can be correlated with the occurrence of both Co and Cd ions in the octahedral position; this ionic distribution increases their susceptability to ammonia uptake. On the other hand, the preferred ionic distribution of Co and Cd ions in the tetrahedral sites rather than in the octahedral ones, explains their lower promotional effects. This seems to be due to the effective isolation of the tetrahedral sites [23] and, thus, a decrease in the ease of formation of the corresponding ammine complex.

Overall, the formation of such an unstable ammine complex first enhances the process of ammonia evolution; then the reaction proceeds

through the suggested mechanism [24]

$$NH_4^+ \longrightarrow NH_3 + H^+ \quad (2)$$

$$H^+ + NO_3^- \longrightarrow HNO_3 \quad (3)$$

$$2HNO_3 \longrightarrow NO_2^+ + NO_3^- + H_2O \quad (4)$$

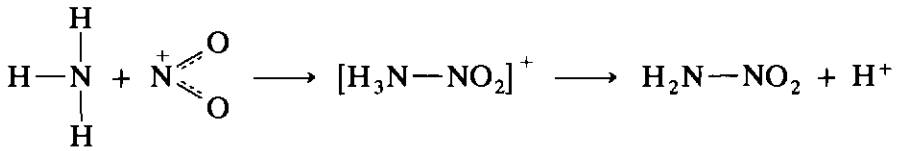

(5)

Thereafter, the nitramide isomerises into nitric acid imide

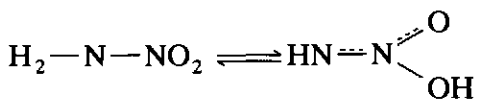

(6)

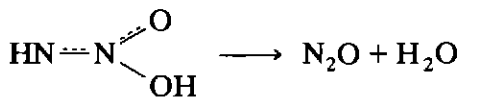

(7)

$$N_2O + 2O_2 \longrightarrow N_2O_5 \quad (8)$$

The protons resulting from NH_4^+ dissociation (eqn. (1)) tend to interact immediately with nitrate ions forming nitric acid (eqn. (3)) which decomposes readily through eqns. (4)–(8) to give, finally, N_2O or N_2O_5. The formation of N_2O_5, either from HNO_3 decomposition or from the residual oxynitrato anion $CeO(NO_3)_2$

$$2NO_3^- \rightarrow N_2O_5 + O^{2-} \quad (9)$$

enhances the formation of Ce=O bonds [12].

In order to relate the promotional behaviour of the catalyst additives to a parameter indicative of their catalytic activity, the patterns of the kinetic (α, t) data exhibited by the different catalysts constituting the present study were analysed and are summerised in Fig. 5b and 5c. A computer-oriented kinetic analysis was also performed, as in the case of the pure sample, and the results indicate that the decomposition process obeys the Avrami–Erofe'ev equation [25], where the nucleation-and-growth mechanism can be put forward to describe the thermal decomposition of DAHC in the presence of catalyst additives. The activation energy values, as indicative kinetic parameters, were also obtained using the Arrhenius equation. The values are $E_a = 58.0$, 53.8 and 44.6 kJ mol^{-1} for the catalysts with $x = 1.0$, 0.0 and 0.5 respectively. The observed reduction in activation energy values, in ascending order $x = 0.0$, 1.0 and then 0.5, parallels the promotional effect of the catalysts, where $x = 0.5$ has the maximum activity.

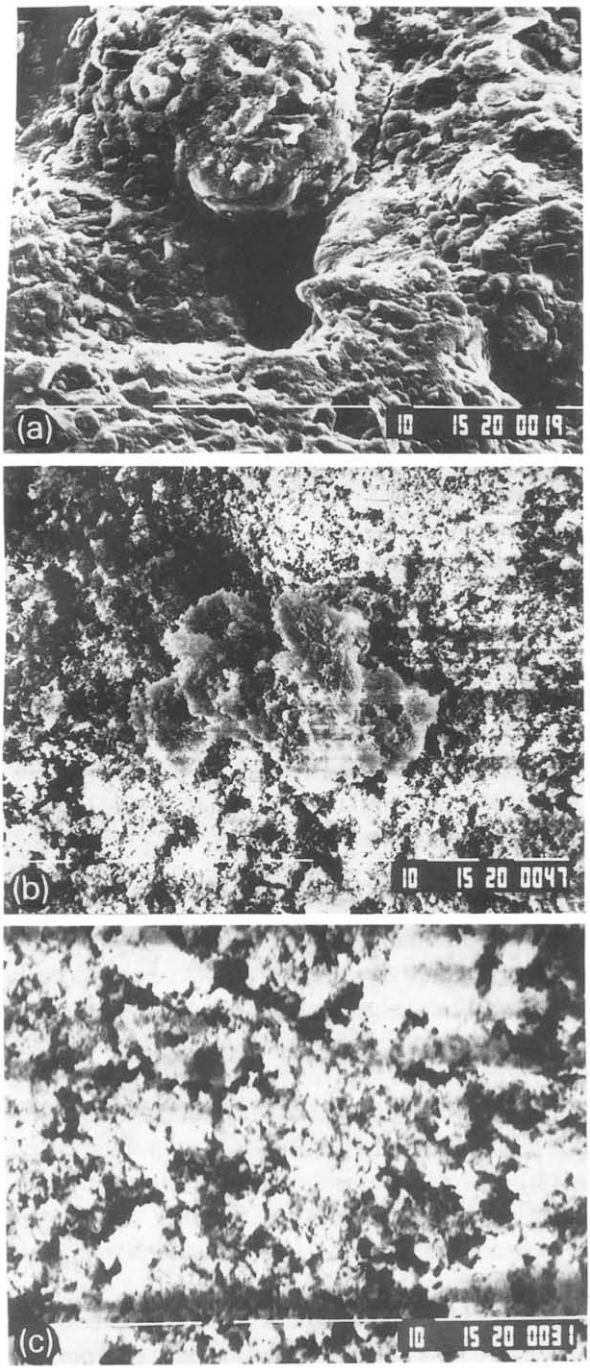

Fig. 7. Scanning electron micrographs for DAHC mixed with 10% (wt/wt) $CdFe_2O_4$ catalyst calcined at 250, 275 and 300 °C (a–c respectively).

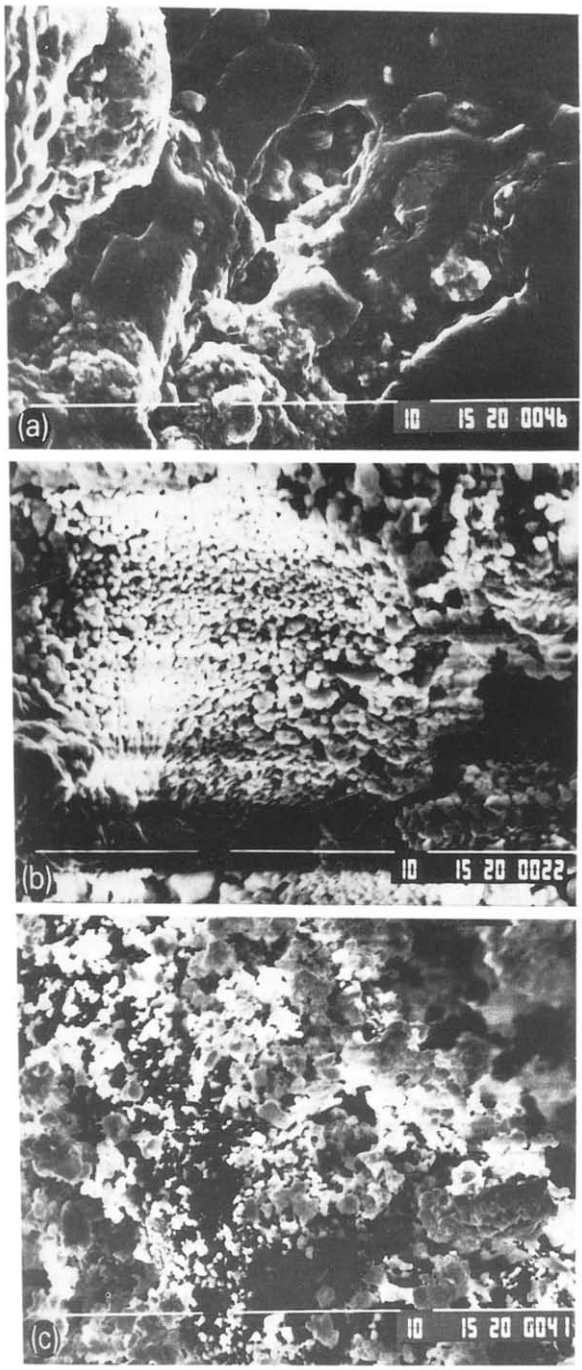

Fig. 8. Scanning electron micrographs of DAHC mixed with 10% (wt/wt) $CoFe_2O_4$ catalyst calcined at 250, 275 and 300 °C (a–c respectively).

The SEM photographs for DAHC mixed catalyst, calcinated at different temperatures, are shown in Figs. 7 and 8. Regarding the texture in these photographs, there is some surface roughening and a local development of the textural features of the solid product, which adheres to the surface, see Figs. 7b and 8b. This can be identified as a nucleus composed of a coherent, asymmetric region of product extending along the surface; the adjacent areas in the photographs are apparently undecomposed salt. These microscopic observations, together with the kinetic conclusions, provide good evidence that in the presence of catalyst additives, the decomposition reaction proceeds by a nucleation-and-growth mechanism, where the product may move through the dislocation network of the reactant and "activate" potential nuclei. This surface stress deformation represents an important factor in the production and development of nuclei.

REFERENCES

1 K.C. Talyor, J.R. Anderson and M. Boudart, Catalysis—Science and Technology, Vol. 5, Springer-Verlag, Berlin, 1984, p. 120.
2 A. Overs and J. Riess, J. Am. Ceram. Soc., 65 (1981) 606.
3 T. Kudo and H. Obayashi, J. Electrochem. Soc., 122 (1975) 142.
4 R.B. Fahim, M.I. Zaki and R.M. Gabr, J. Chem. Technol. Biotechnol., 30 (1980) 535.
5 M.I. Zaki and N. Sheppard, J. Catal., 80 (1983) 114.
6 J.W. Mellor, A Comprehensive Treatise on Inorganic and Theoretical Chemistry, Vol. 5, Longmans, London, 1960, p. 625.
7 R. Blumenthal, P.W. Lee and R.J. Panlener, J. Electrochem. Soc., 118 (1971) 123.
8 C.H. Bamford and C.F.H. Tipper, Comprehensive Chemical Kinetics, Vol. 22, Elsevier, Amsterdam, 1980, p. 115.
9 A.M. El-Awad, R.M. Gabr and M.M. Girgis, Thermochim. Acta, 184, 2 (1991) 205.
10 A.K. Galwey, Proc. 7th Int. Conf. Therm. Anal., (1982) 38.
11 R.M. Gabr, A.M. El-Awad and M.M. Girgis, J. Therm. Anal., 37 (1991) 249.
12 M.I. Zaki and T. Baird, Reactivity of Solids, 2 (1986) 107.
13 F.A. Miller and C.H. Wilkins, Anal. Chem., 24 (1952) 1253.
14 J.R. Ferraro, J. Inorg. Nucl. Chem., 10 (1959) 319.
15 M. Terada and M. Tsuboi, Bull. Chem. Soc. Jpn., 37 (1964) 1080.
16 K.N. Ninan and C.G.R. Nair, Thermochim. Acta, 30 (1979) 25.
17 P.D. Garn, in H. Kambe and P.D. Garn (Eds.), Thermal Analysis: Comparative Studies on Materials, Wiley, New York, 1974, p. 100.
18 L.G. Harrison, C.H. Bamford and C.F.H. Tipper, Comprehensive Chemical Kinetics, Vol. 2, Elsevier, Amsterdam, 1969, Chap. 5.
19 A.K. Galwey, D.M. Jamieson, M.E. Brown and M.J. McGinn, Reaction Kinetics in Heterogenous Chemical Systems, Elsevier, Amsterdam, 1975, p. 520.
20 R.M. Gabr, M.M. Girgis and A.M. El-Awad, in press.
21 A.E. Wells, Structural Inorganic Chemistry, 4th edn., Clarendon Press, Oxford, 1975, p. 957.
22 H. Kambe and P.D. Garn, Thermal Analysis: Comparative Studies on Materials, Halsted Press, Kodansha Ltd, Tokyo, 1974, p. 17.
23 A.I. Onuchukwu and A.B. Zuru, Mater. Chem. Phys., 15 (1986) 131.
24 Z.G. Szabo, E. Hollos and J. Trompler, Z. Phys. Chem. Neue Folge, 144 (1985) 187.
25 A.K. Galwey and M.A. Mohamed, J. Chem. Soc. Faraday Trans. 1, 81 (1985) 2503.